論文 / 著書情報
Article / Book Information

Title	Survival of young planted mangroves in a calm bay environment during a tropical cyclone
Authors	Hiroshi Takagi
Citation	Nature-Based Solutions, Vol. 4, ,
Pub. date	2023, 8
DOI	https://doi.org/10.1016/j.nbsj.2023.100082
Creative Commons	Information is in the article.

Nature-Based Solutions 4 (2023) 100082

Contents lists available at ScienceDirect

Nature-Based Solutions

journal homepage: www.elsevier.com/locate/nbsj

Survival of young planted mangroves in a calm bay environment during a tropical cyclone

Hiroshi Takagi

School of Environment and Society, Tokyo Institute of Technology, Japan

ARTICLE INFO

Keywords:
Mangrove plantation
Typhoon
Survival rate
Amami Island
Plant oscillation
Short-period waves
Tide level
Nature-based solution
Green infrastructure
Numerical simulation

ABSTRACT

The efforts of mangrove plantations are not always successful, and the reasons for their failure remain unclear. In this study, the growth of planted mangroves (*Kandelia sp.*) was monitored in a mangrove forest on Amami Island, Japan, to investigate their survival over the first three years. A strong typhoon passed near the island 16 months after planting. Although the mangroves were planted at the frontal edge of the intertidal zone, most of young mangroves survived without visible damage. The external forces acting on the plants, such as wave forces, storm surge forces, wind drag forces, and oscillatory acceleration, were estimated by applying an integrated analysis model for tropical cyclones, storm surges, wind waves, and plant kinematics. These analyses yielded three main results. First, although large waves over 10 m in height were generated offshore, the mangrove forest was located in the innermost part of the bay, resulting in considerable wave attenuation. Second, the wave period in the bay was much shorter than that in the open ocean, which may have promoted resonance between waves and mangrove plants. The oscillatory acceleration of the young mangroves was estimated to have approximately the same magnitude as that of the gravitational force. Third, the young mangroves could withstand a fairly strong typhoon, but this may have been fortuitous because the timing of the adverse wind wave conditions coincided with low tide. It is estimated that if the tides had been higher, the oscillatory acceleration would have been five times that of the gravitational acceleration. Although this study only presents examples of specific mangrove species in a particular location, the findings can be used to improve the attempts to restore mangrove forests and thereby protect coastal settlements from the adverse effects of tropical cyclones.

1. Introduction

In recent years, the concepts of natural-based solutions (NbS), [1] Ecosystem-based Disaster Risk Reduction (Eco-DRR), [2] and green infrastructure (GI)[3] have attracted considerable attention as means of coastal disaster mitigation or climate change adaptation using coastal and estuarine ecosystem services [3,6,11,12,29,33,53]. One of the impetuses of this concept is the identification of settlements protected by the presence of mangroves along the coast of countries such as India, Thailand, and Sri Lanka, which were severely affected by the Indian Ocean tsunami in 2004 [1,2,14]. Many lives were lost in coastal villages without mangrove forests, whereas the number of deaths was remarkably lower in villages shielded by mangrove forests [2,14,27]. Previous surveys have also shown that coastal areas in the Philippines, USA, and New Zealand that were affected by storm surges induced by tropical cyclones have been protected by the presence of mangroves [34, 36]. However, other studies have suggested that mangroves have a limited effect on attenuating tsunamis and storm surges or that this effect can only be expected if the mangrove forest is sufficiently wide [1, 43,51]. Mangrove-inhabited coastal environments promote intertidal sedimentation because (1) they dissipate hydrodynamic energy, (2) they are important sites for organic matter production, and (3) they contain flora and fauna that influence sediment composition [30,41]. Despite this plausible coastal geomorphology theory, an analysis of the Indian

E-mail address: takagi.h.ae@m.titech.ac.jp.

[1] Nature-based solutions (NbS) are defined as actions to protect, sustainably manage, and restore natural or modified ecosystems, which address societal challenges effectively and adaptively, simultaneously providing human well-being and biodiversity benefits [22].

[2] Ecosystem-based disaster risk reduction (Eco-DRR) is a concept to reduce the risk of being exposed to natural hazards by avoiding development of disaster-prone areas, as well as by using healthy ecosystems as buffers, to protect people's living and properties [35].

[3] Green infrastructure (GI) is an interconnected network of green space that conserves natural ecosystem values and functions to provide associated benefits to human populations [4].

https://doi.org/10.1016/j.nbsj.2023.100082
Received 29 April 2023; Received in revised form 31 July 2023; Accepted 1 August 2023
Available online 2 August 2023

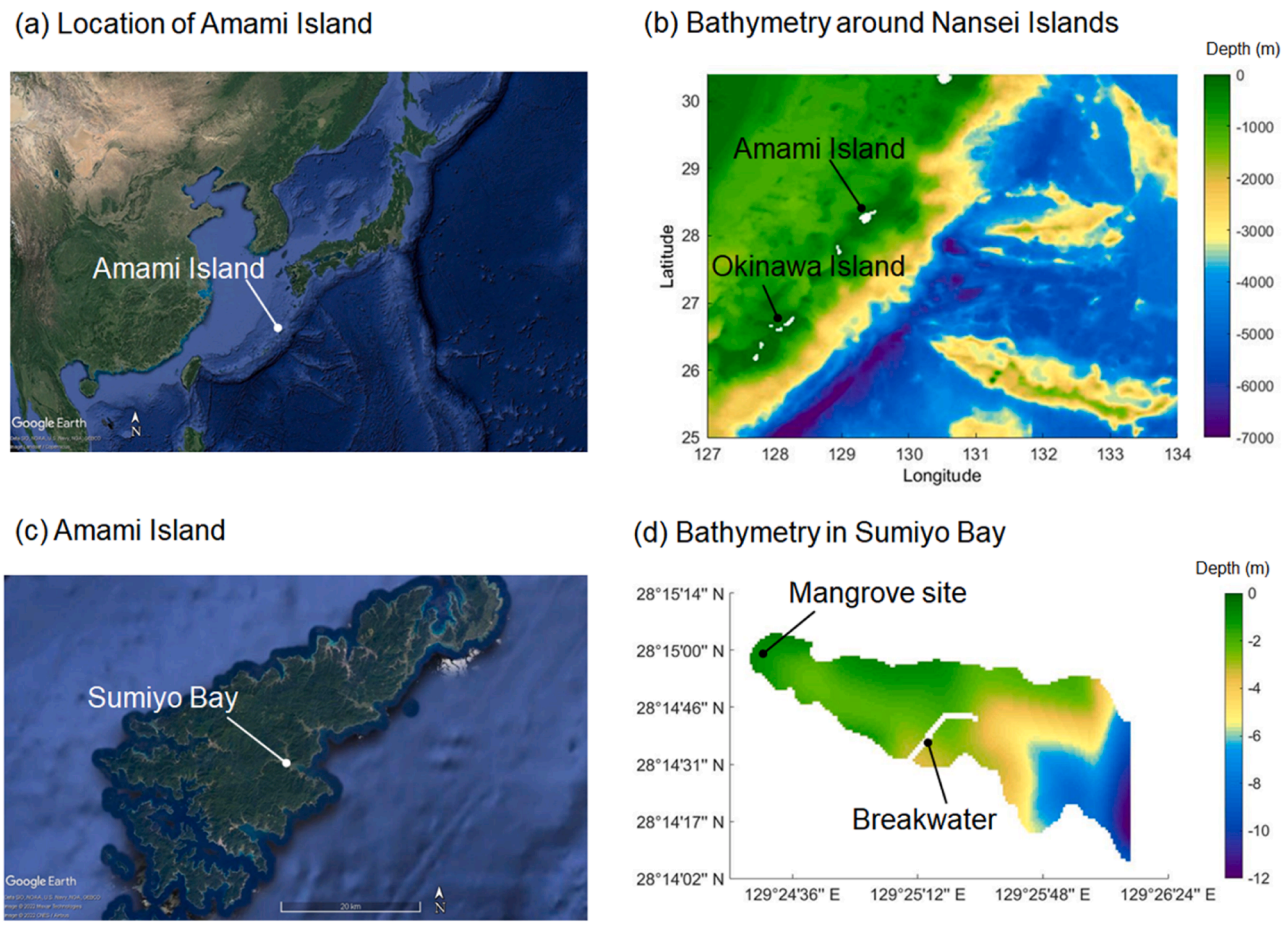

Fig. 1. Location and bathymetry maps of Amami Island and Sumiyo Bay. Amami is the largest island in the Amami Archipelago, located between Kyushu and Okinawa. Sumiyo Bay is a long and narrow bay with natural mangrove forests in the inner-most shallow water into which two rivers flow.

coast showed that coastal erosion has not slowed remarkably, even if mangrove plantations are implemented [9]. Although the evidence is not conclusive, some of these past successes appear to be strong drivers of NbS, Eco-DRR, and GI.

Mangrove forests have been reduced due to aquaculture, such as shrimp farming, conversion to rice cultivation, charcoal production, palm oil plantations, infrastructure construction, and urbanization [37,39,44,66]. Mangrove forests that existed in 2000 were reduced by 1646 km^2 worldwide by 2012. This corresponds to a 1.97% decrease in the total area in 2000 [17]. In addition to anthropogenic factors, mangrove forests in the Philippines and the Bahamas have been severely damaged by Typhoon Haiyan in 2013 and Hurricane Durian in 2019 [65,67]. Planting only certain mangrove species, such as *Rhizophora*, may lead to large-scale losses due to such extreme events [65]. As these mangrove shields are destroyed, the coastline becomes more vulnerable, and the carbon stored in these ecosystems is released back into the atmosphere, further contributing to anthropogenic climate change [12]. Deforested mangrove areas adversely affect fisheries [10] and accelerate coastal erosion [7].

To compensate for the decline in mangroves, regional mangrove plantation projects are being undertaken to restore mangrove forests that have been cut down, especially in the Asian region. These projects have been implemented by governments, non-governments, and non-profit organizations [9,42,43]. Despite such regional efforts, however, many attempts to rehabilitate mangroves have failed completely or achieved their original goals [31]. For example, in the Philippines, the long-term survival rate of mangroves is only 10–20% despite the huge amount of money invested in mangrove forest plantations in recent decades. Mangroves planted in the Central Visayas between 1984 and 1992 had an average survival rate of 18% as of 1995 [42]. Similarly, the success rates of reforestation programs were only 25% in Vietnam and from 0 to 78% in Sri Lanka [21,28]. For the Sri Lankan study, success was defined as survival for a minimum of five years, but for the Vietnamese study, the criteria for monitoring duration are unknown. In Thailand, the definition of targets was ambiguous, and officials reported "false success" based on the land area planted, not on the long-term survival rate of planted mangroves [62].

Young mangroves are generally vulnerable to barnacles, waves, inappropriate soil conditions, and pollution such as plastic waste [28,64]; however, because of the lack of scientific knowledge on reforestation measures, mangrove planting is often performed on a trial-and-error basis [16]. Survival is also significantly correlated with the post-care of mangrove seedlings [28]. In particular, because mangroves take a certain amount of time to grow, large waves during the initial stage could wash away planted mangrove seedlings [46]. For example, in the case of plantations of *Kandelia obovata* in Vietnam, it was recorded that it took 5 years to grow approximately 1.2 m, 10 years to grow 2.2 m, and 20 years to grow 4.6 m [8]. To increase the success rate of mangrove plantations, empirical attempts have been made to reduce waves in plantation areas using improvised methods such as rubble mounds, wooden piles, and brushwood fences [26,47,55,61,66]. Although there have been some successes in local community participation in mangrove plantations, they are often poorly documented and cannot be applied to other projects [40]. Consideration of the balance between ecology and engineering is also limited [13,47,53].

Unlike hard engineering structures that start functioning immediately after completion, nature-based solutions may not function as disaster mitigation measures during the initial plant growth phase, and

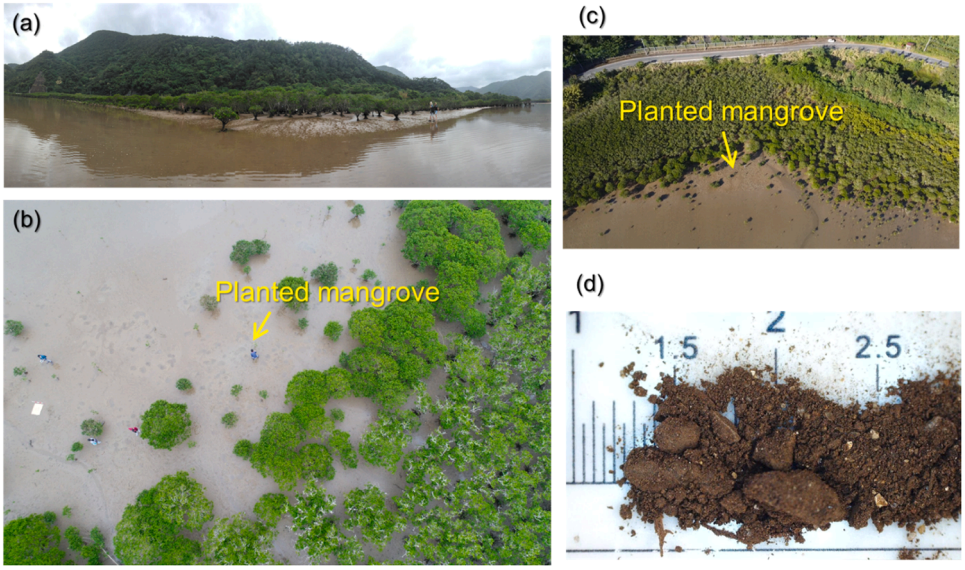

Fig. 2. Mangrove forest of the study site, the location of the planted mangrove growth test, and local soils. Seven mangroves were planted on the seaward edge of the forest. This mangrove forest is not considered a primary forest because it has developed along the coastal road.

it is necessary to realize this constraint. Sreeranga et al. [46] found that the initial stage of six months to a year is a particularly important period for young mangroves (*K. obovata*) to become able to withstand normal waves. Guidance regarding the design conditions for the external forces acting on the system is also lacking. Thus, despite the advantages of the NbS, Eco-DRR, and GI concepts, there is a lack of concrete guidance on the extent to which these measures are effective and on their practical design [46,53,59].

This study aimed to monitor the growth of seven planted mangroves in a mangrove forest on Amami Island, Japan, to investigate their survival over the first three years. During this period, a strong typhoon approached the island, providing the opportunity to study various levels of external forces affecting young mangroves. The findings of this study may provide a concrete example of how long young mangroves need to be protected in an engineered manner, which will be fundamental in designing science-based ecosystem disaster-mitigation strategies.

2. Methods and data

This section provides an overview of the mangrove forests on Amami Island and the mangrove growth tests conducted. Numerical simulations of wind, waves, and storm surges were performed to evaluate the external forces acting on planted mangroves during typhoons. In addition, a method for calculating the oscillation of young mangroves caused by waves is described.

2.1. Study site and mangrove growth test

In this study, a growth test of *K. obovata* (*K. candel*) was conducted in a native mangrove forest on Amami Island, located in the Nansei Islands of Japan (Fig. 1). The growth of seven planted mangroves was monitored to investigate their survival over the first three years. Four field surveys were conducted from May 2019 to May 2022. Mangrove forests, approximately 4 km long and narrow, are present in the innermost part of Sumiyo Bay. Although the water depth is generally shallow throughout the bay, mangroves thrive only in the estuary and along the coastline, where muddy sediments are substantially deposited (Fig. 2). Two mangrove species, *K. obovata* and *Bruguiera gymnorhiza*, grow in this forest, with the height of the mature trees being approximately 3 to 4 m. Among the two species, *K. obovata* is particularly dominant. The forest is expanded in a brackish area where salinity remarkably

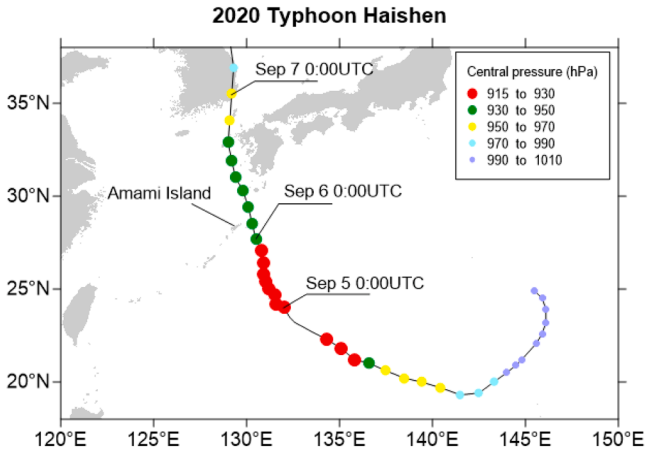

Fig. 3. Path and central pressure of Typhoon Haishen in 2020. This typhoon was one of the strongest typhoons in the 2020 Pacific typhoon season.

fluctuates due to the seasonal difference in river flows (8‰ to 22‰ according to our field survey). Interestingly, this mangrove forest has developed along the coastal road (Fig. 2**c**), which is an ideal location to consider integrating NbS with the existing infrastructure. The historic size and range of this forest is not clear, but aerial photographs from the 1960s and 1970s indicate that the forest already existed in the same location. However, the recent extent of the mangrove range seems to have extended a little further along the coastal road.

Mangroves are usually widespread in the intertidal zone between mean tide and mean high tide [23,32] but are more severely affected on the ocean-side forest fringe with respect to survival because of direct exposure to waves. To investigate the survival of mangroves in severe environmental conditions, a mangrove growth test was conducted by planting the collected propagules (seeds) of *K. obovata* at the ocean-side edge of the forest (Fig. 2). The topography of this mangrove forest is roughly a 1/100 slope, and the ground is sometimes submerged and sometimes completely dry, depending on the tide level. The soils of the mangrove forests are mostly fertile fine silt and do not contain sand, but small stones of a few millimeters in size are sparsely present (Fig. 2).

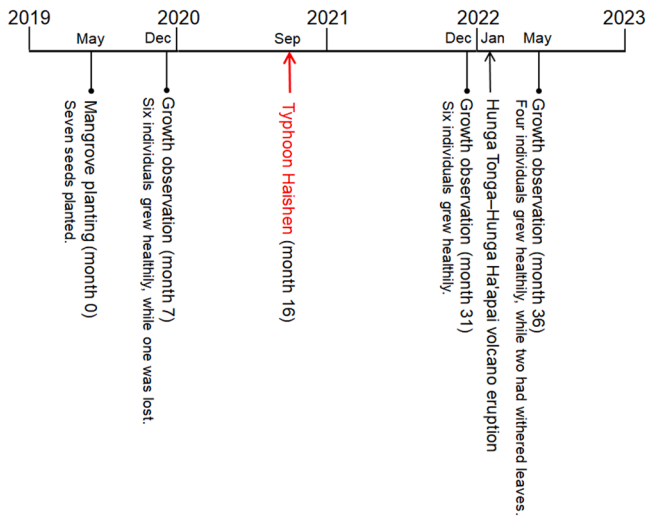

Fig. 4. Time series of mangrove growth test on Amami Island: timing of the survey, disaster events, and mangrove survival status. Typhoon Haishen occurred 16 months after planting.

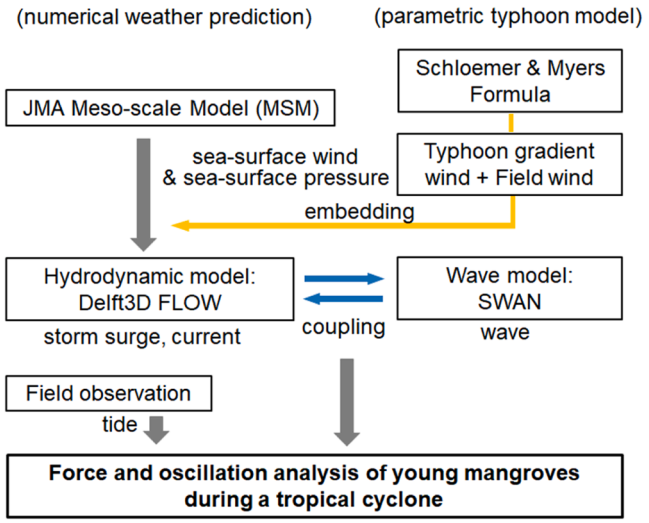

Fig. 5. Coupled weather, wind wave, and storm surge model to evaluate external forces acting on mangroves. Tides were estimated based on field surveys in the mangrove forest. The oscillation analysis calculates the horizontal acceleration due to waves acting on the plant.

2.2. Typhoon event during the growth test

Approximately 25 typhoons occur in the Northwest Pacific each year, of which 12 approach Japan and three eventually make landfall [25,58]. The Nansei Islands, including Amami Island, are the areas most frequently approached by tropical cyclones in Japan; however, because the islands are scattered, the chance of the closest approach of very strong typhoons is not necessarily high. Among the 621 typhoons that occurred between 1990 and 2013, only 17 had a central pressure of 935 hPa or less, approaching closest to the islands [49]. Typhoon Haishen in 2020 was one of the strongest typhoons of recent years, with a central pressure of 930 hPa when it passed near Amami Island (Fig. 3). This typhoon was the only one that passed within 100 km of the island during the three years of the mangrove growth test (16 months after planting) (Fig. 4).

2.3. Numerical modeling of typhoon, wave, and storm surge

A numerical analysis of the wind waves and storm surges caused by Typhoon Haishen was performed using the model developed by Takagi and Takahashi [57], as shown in Fig. 5. For weather input, this model used data provided by the Japan Meteorological Agency (JMA), referred to as the JMA's mesoscale numerical model [24]. The computational domain covered Japan and the surrounding areas (4080 × 3300 km), with 48 vertical layers (the lowest layer was 10 m above the surface). The JMA's mesoscale numerical model was constructed on a computational grid with a horizontal resolution of 5 km, which was insufficient to model the steep pressure gradients of typhoons. Therefore, in the present model, the center of the typhoon and its vicinity were replaced by an empirically determined parametric typhoon model (the Schloemer and Myers Formula, which is well established and commonly used in storm surge models) [38,45]. The typhoon center locations were obtained from the best track data of the JMA every three hours and interpolated into hourly latitudes and longitudes.

By inputting typhoons and the surrounding atmospheric fields, wind-generated waves were simulated using the Simulating Waves Nearshore (SWAN) model, which is a third-generation wave model that computes random waves in coastal regions [63]. Simultaneously, hydrodynamic analysis was performed using Delft3D FLOW, a hydrostatic nonlinear shallow water solver that computes unsteady flow, and the results were communicated with SWAN every 60 min. This integrated model can simulate many hydrodynamic parameters such as wave height/period, storm surge level, and flow velocity. The reliability of the model has been verified for past strong typhoons over the Western North Pacific, such as Haiyan in 2013 [48,50], Goni in 2015 [49], Hato in 2017 [52], and Faxai in 2021 [57].

The simulation domain comprised a wide area that included most of the Nansei Islands, and a narrow area that focused on Sumiyo Bay on Amami Island. For a wide area, bathymetry data from the General Bathymetric Chart of the Oceans (GEBCO) were used in the computation as gridded data with a 0.02 arc-degree (approximately 2.2 km) interval. Because no public electrical bathymetry data exist for the shallow water area of Sumiyo Bay, approximately 24 m of grid data were created based on paper nautical charts. An erosion-control weir that functioned as a breakwater was constructed on the southern side of the center of the bay, creating a calm wave environment (Fig. 1). Hence, the bathymetry data were manually modified to reflect this breakwater (approx. 600 m extension).

The SWAN model accounts for most wave physics, including wave refraction, shoaling, breaking, and dissipation. Several options were selected for better simulation, including the Komen model for wave generation and the Battjes–Janssen model for wave breaking. For the roughness of the seafloor, Manning's n value of 0.02 (s $m^{-1/3}$) was used for the entire computational domain [54]. To account for wave attenuation in the shallow-water areas of the bay, an empirical frictional resistance equation, the JONSWAP bottom friction model [18], was also used. Radiation stress can also be calculated; however, simulations on coarse grids rarely reflect the effects of wave setups in shallow water, such as the water in mangrove forests.

The astronomical tide can also be simulated in Delft3D FLOW, but it may not be sufficiently reliable because it is sensitive to subtle variations in local elevation around the mangrove forest located at the far end of the bay. Therefore, the astronomical tide levels during the typhoon were separately assumed based on the results of field observations (see Appendix A1).

2.4. Theory of forces acting on young mangroves

Young mangroves respond flexibly to oscillating waves, thereby preventing damage. However, if the oscillation is too strong, leaves that are not sufficiently strong may fall. Takagi et al. [56] modeled the oscillatory responses of young mangroves by assuming a single degree of

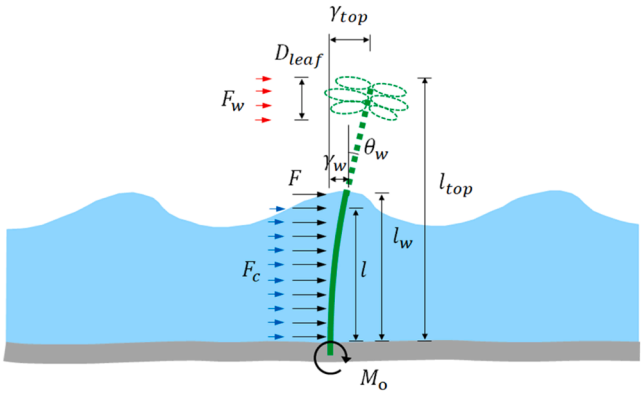

Fig. 6. Deflection of a young mangrove subject to wave force F, current F_c, and wind force F_w. The combined force of the three forces is assumed to act in the same direction.

freedom, as described in the following second-order ordinary differential equations for time t, considering various factors such as plant strength, wave height, wave period, and water depth.

$$\frac{d^2\gamma}{dt^2} + 2h\omega_0\frac{d\gamma}{dt} + \omega_0^2\gamma = \frac{F}{m}\cos\omega t \tag{1}$$

where γ is the horizontal displacement of an oscillatory body, m is the mass, F is the amplitude of the wave force, ω is the angular frequency of the wave, ω_0 is the natural angular frequency of an object, and h is the viscosity damping constant.

The horizontal displacement γ_w at the water surface and γ_{top} at the plant tip, as shown in Fig. 6, can be calculated by the following equations.

$$\gamma_w = \frac{pl_w^4}{8EI} \tag{2}$$

$$\gamma_{top} = \gamma_w + (l_{top} - l_w)\tan\theta_w \tag{3}$$

where p is the wave pressure, l_w is the length under the water surface, E is Young's modulus, I is the second moment of the area, and θ_w is the deflection angle. Zhang et al. [68] showed that the prop roots of mature mangroves subjected to dynamic tidal loading had a large Young's modulus E of approximately 15 GPa. Because this study was conducted on young mangroves, and the stiffness should be much smaller, one-tenth of this value (1.5 GPa) was assumed.

In contrast, the wave force can be calculated using the following equation [56].

$$F = \left(\frac{1}{2}\rho C_D \phi u_w \cos\frac{2\pi t}{T}\left|u_w\cos\frac{2\pi t}{T}\right| - \frac{1}{4}\rho C_M \pi\phi^2 u_w \frac{2\pi}{T}\sin\frac{2\pi t}{T}\right) l_w \tag{4}$$

$$l_w = l + \frac{H}{2}\cos\frac{2\pi t}{T} \tag{5}$$

where T is the wave period, ρ is the water density, ϕ is the plant diameter, u_w is the fluid velocity induced by the waves, and C_D and C_M are the drag and mass coefficients, respectively (For the estimation for C_D and C_M, refer to Takagi et al. [56]). l_w changes with time t with respect to still water depth l (Fig. 6) and wave height H.

Although there are various definitions for ocean irregular wave heights and periods, in this study, the significant wave height (average of the top 1/3 of the wave heights) and peak period (peak period of the energy spectrum) were used as H and T.

The fluid velocity u_m and maximum horizontal displacement of the water particle ζ_{max} can be approximated using the following equations:

$$u_m = \frac{gkHT}{4\pi} \tag{6}$$

$$\zeta_{max} = \frac{1}{2}\frac{H}{\tanh kl} \tag{7}$$

where g is the gravitational acceleration and k is the wave number, which can be calculated using the following equation [15].

$$k = \frac{\sigma^2}{g\sqrt{\tanh\left(\frac{\sigma^2}{g}h\right)}} \tag{8}$$

Note that the flow velocity decreases with depth, but Eq. (6) is independent of water depth. This is because mangroves grow in very shallow water and the velocity is assumed to be constant across water depth [56].

The second-order ordinary derivative of Eq. (1) can be solved as follows [56].

$$\gamma_w = -Ae^{-h\omega_0 t}\left(\cos\alpha\cos\omega_D t + \left(\frac{\omega}{\omega_D}\sin\alpha + \frac{h}{\sqrt{1-h^2}}\cos\alpha\right)\sin\omega_D t\right) + A\cos(\omega t - \alpha) \tag{9}$$

where $\omega_D = \sqrt{1-h^2}\omega_0$, meaning that if the damping constant h is small, the period of oscillation of a plant becomes closer to the natural period of oscillation T_0 $\left(=\frac{2\pi}{\omega_0}\right)$. In this study, T_0 was assumed to be 0.36 s, based on the experimental results reported by Takagi et al. [56].

The amplitude A and phase α are expressed by the following equations,

$$A = \frac{Fl^3}{4EI\sqrt{\left(1-\left(\frac{\omega}{\omega_0}\right)^2\right)^2 + 4h^2\left(\frac{\omega}{\omega_0}\right)^2}} \tag{10}$$

$$\alpha = \tan^{-1}\left(\frac{2h\left(\frac{\omega}{\omega_0}\right)}{1-\left(\frac{\omega}{\omega_0}\right)^2}\right) \tag{11}$$

Using these parameters, Takagi et al. [56] defined the wave-induced oscillatory amplification of young mangroves, D_{amp}, as the ratio of the orbital amplitudes of water particles, using the following equation:

$$D_{amp} = \frac{\gamma_{top}}{\zeta_{max}} \tag{12}$$

The higher the value, the greater the amplitude of the stems shaken by the waves. In particular, the values of D_{amp} were found to be significantly larger when the natural frequency period of the young mangrove was the same as or a multiple of the wave period.

As shown in Fig. 6, all forces acting on the mangrove resulted in a bending moment of M_o around the base of the stem. The following equation expresses the bending moment owing to waves:

$$M_{o\_wave} = \frac{1}{2}Fl_w \tag{13}$$

In addition to waves, storm-induced currents and winds also exert forces on young mangroves during typhoons.

$$M_{o\_current} = \frac{1}{2}F_c l \tag{14}$$

$$F_c = \frac{1}{2}\rho_w C_D u_c^2 \phi l \tag{15}$$

where $M_{o\_current}$ and F_c are the bending moment and drag force induced by the current, respectively; and u_c is the flow velocity induced by the storm surge. ϕ is the diameter of the mangrove stem, assumed to be 10

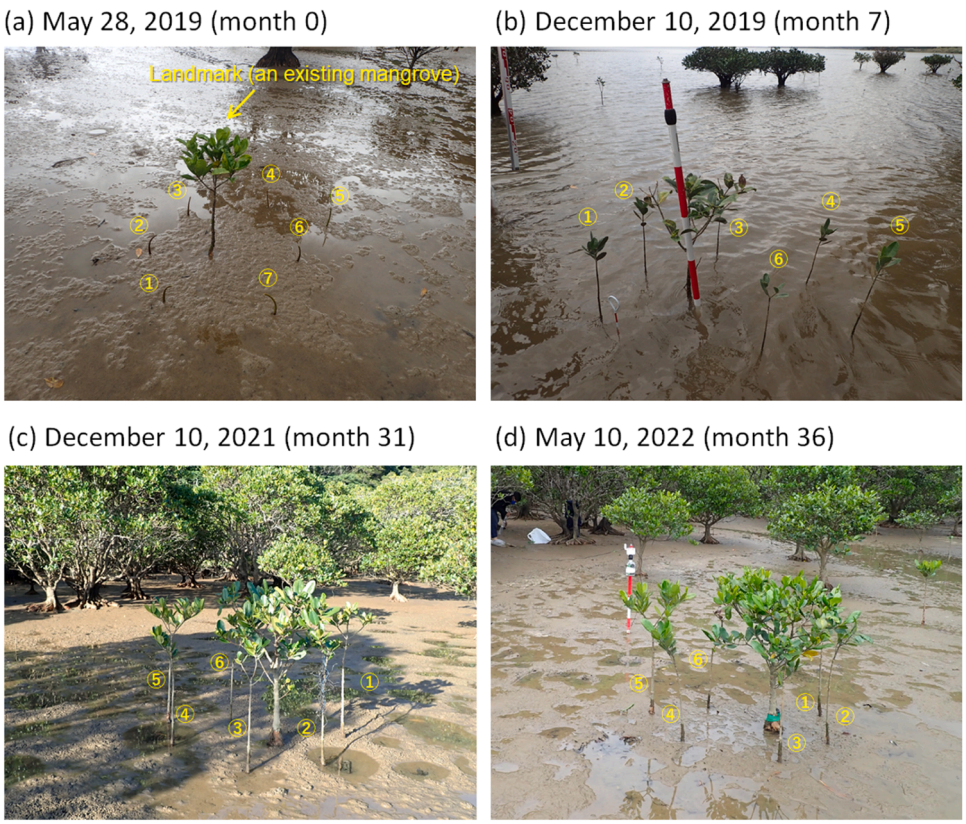

Fig. 7. Observation of mangrove growth for 3 years in Sumiyo Bay, Amami, Japan. Seven mangroves were planted, of which six survived after three years.

mm based on the survey. The value of C_D was assumed to be 1.0 with reference to the drag coefficient of the cylindrical piles.

In the case of wind, the wind force was assumed to act on the projected area, as shown in Fig. 6, because it was concentrated in the leaf area. The bending moment due to wind acting on the leaf was calculated using the following equation:

$$M_{o\_wind} = F_w\left(l_{top} - \frac{1}{2}D_{leaf}\right) \tag{16}$$

$$F_w = \frac{1}{8}\rho_a C_D w^2 \pi D_{leaf}^2 \tag{17}$$

where M_{o_wind} and F_w are the bending moment and drag force induced by the wind, respectively; w is the wind speed; and ρ_a is the air density. D_{leaf} is the radius of the projected area and was assumed to be 20 cm based on field observations.

3. Results

The growth of mangroves was estimated based on the three-year observations of the planted mangroves. The numerical simulation results of wind, waves, and storm surges acting on young mangroves during Typhoon Haishen are then described.

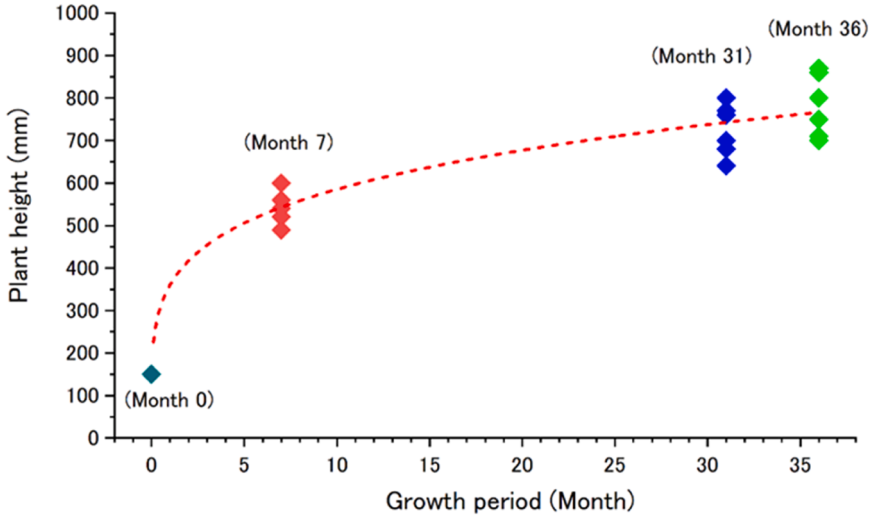

Fig. 8. Relationship between growth period and plant height. In the second year, the observation could not be conducted due to the Covid-19 outbreak.

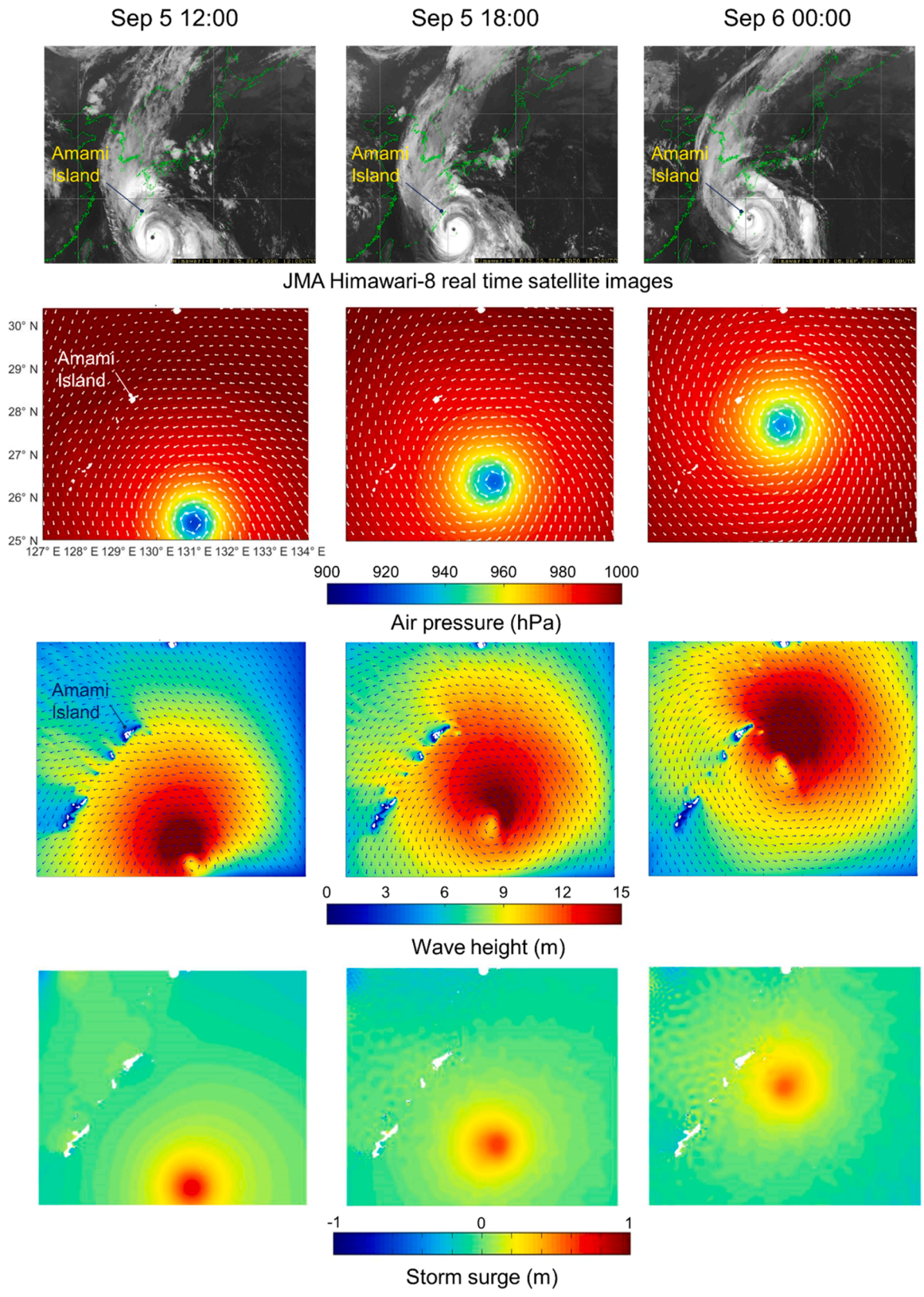

Fig. 9. Comparison of satellite images and simulated sea-level air pressure, wave height, and storm surge at the time of Typhoon Haishen's approach to Amami Island. The spatial extent of the satellite imagery ranges from 114°E to 160°E and 17°N to 52°N, while the numerical analysis ranges from 127°E to 134°E and 25°N to 30.4°N.

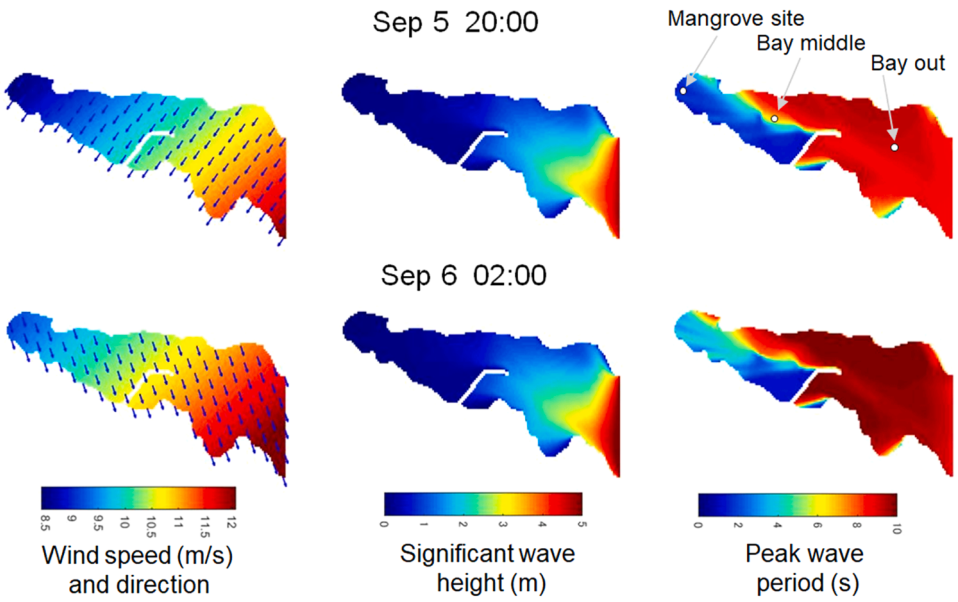

Fig. 10. Simulation outputs with respect to wind speed, wave height, and wave period. The maximum wave height was on September 5 at 20:00, and the maximum wave period was on September 6 at 02:00.

3.1. Observation of mangrove growth

In May 2019, seven seeds with an average length of 19 cm (±2 cm) were planted around an easily discernible mangrove (Fig. 7). Subsequently, planted mangroves were observed in December 2019, December 2021, and May 2022 to monitor their growth and survival rates over a three-year period. At this site, the topsoil was exposed to low tide and was submerged up to 1 m at high tide (see Apendix A1).

Seven months after planting, one of the seven mangroves disappeared for unknown reasons. Six plants survived for 31 months in good condition; however, after 36 months, withered leaves were observed in two of the mangroves. As shown in Fig. 4, Typhoon Haishen occurred 16 months after planting, indicating that the typhoon did not cause any external damage to the six mangroves.

The growth of the mangrove in the initial three years is shown in Fig. 8, and the growth curve can be represented by the following allometric equation:

$$(plant\ height\ in\ mm) = 360 \times (growth\ period\ in\ month)^{0.21} \quad (18)$$

Although field surveys were not possible in 2020 owing to the spread of Covid-19, the average mangrove height above ground was estimated to be 650 mm by applying this equation to 16-month mangroves when Typhoon Haishen hit Amami Island in September 2020.

3.2. Estimated result of waves off the coast of Amami Island

Fig. 9 shows a comparison of the JMA satellite images with the simulated sea-level air pressure and wave height when Typhoon Haishen approached Amami Island. The center of the typhoon did not pass directly over the island but moved approximately 100 km offshore to the east. The translational speed at 12 h was approximately 22 km/h, which is the average speed of a typhoon. The eye of the typhoon was clear, and the central pressure was very low at 930 hPa during the closest approach. Waves were particularly high ahead of the typhoon's travel direction and were estimated to be up to 15 m high. Waves 10 m high were estimated to have been generated off Amami Island during the course of the typhoon. The direction of the waves was initially from the east but changed to be from the north in a short time. The typhoon moved over deep water (1000–3000 m), an environment prone to high waves. In contrast, storm surges are less likely to develop because of the deep waters, and the numerical simulation results show that the maximum water level was less than 1 m, even near the center of the typhoon. As the atmospheric pressure drop was approximately 80 hPa (equivalent to an 80 cm water level rise), the storm surge can be mostly attributed to pressure-driven surges rather than wind-driven surges.

Table 1
Various meteorological and hydrological outputs at the mangrove site from 12:00 on September 5 to 6:00 on September 6.

Date / Time (UTC)	Tide * (m)	Pressure drop (hPa)	Storm tide ** (m)	Wind speed (m/s)	Current (m/s)	Significant wave height (m)	Peak wave period (s)
Sep 5 12:00	0.28	16	0.44	6.02	0.025	0.134	1.44
Sep 5 14:00	−0.04	18	0.14	6.28	0.024	0.124	1.46
Sep 5 16:00	−0.49	22	−0.27	6.81	0.028	0.130	1.46
Sep 5 18:00	−0.74	26	−0.48	7.83	0.033	0.140	1.48
Sep 5 20:00	−0.60	28	−0.32	8.51	0.037	0.142	1.48
Sep 5 22:00	−0.17	33	0.16	7.69	0.030	0.087	1.58
Sep 6 00:00	0.25	39	0.64	8.96	0.030	0.066	2.13
Sep 6 02:00	0.39	44	0.83	9.26	0.020	0.054	3.28
Sep 6 04:00	0.23	45	0.68	9.88	0.002	0.049	3.11
Sep 6 06:00	0	37	0.37	8.27	0.013	0.064	1.61

* Tide levels are adjusted from astronomical tide levels to local water levels with reference to observational data and are displayed based on the ground surface (see Appendix A1).
** Storm tide is the combined water level of the astronomical tide and the storm surge due to atmospheric pressure drop.

Table 2
Horizontal forces and bending moments acting on young mangroves during the passage of Typhoon Haishen. The numbers in bold font indicate the maximum value for that parameter.

Date / Time (UTC)	Wave Force (N)	Moment (N m)	Current Force (N)	Moment (N m)	Wind Force (N)	Moment (N m)	Total force (N)	Total moment (N m)
Sep 5 12:00	**0.54**	**0.137**	0.001	0.00	0.74	0.405	1.28	0.542
Sep 5 14:00	0.47	0.047	0.000	0.00	0.80	0.441	1.27	0.488
Sep 5 16:00	Totally exposed to air at low tide level				0.94	0.518	0.94	0.518
Sep 5 18:00					1.25	0.685	1.25	0.685
Sep 5 20:00					**1.47**	**0.809**	**1.47**	**0.809**
Sep 5 22:00	0.21	0.021	0.001	0.00	1.20	0.661	1.41	0.682
Sep 6 00:00	0.10	0.033	**0.003**	0.00	Totally submerged at high tide level		0.10	0.033
Sep 6 02:00	0.07	0.030	0.001	0.00			0.07	0.031
Sep 6 04:00	0.05	0.018	0.000	0.00			0.05	0.018
Sep 6 06:00	0.11	0.022	0.000	0.00	1.39	0.764	1.50	0.786

3.3. *Wind, waves, and storm surge in Sumiyo Bay*

Fig. 10 shows the results of a detailed numerical analysis focusing on Sumiyo Bay on Amami Island, including wind speed and direction, significant wave height, and peak period. The upper figure (Sep 5, 20:00) shows when the waves near the mangrove site were at their highest, whereas the lower figure (Sep 6, 02:00 a.m.) shows when the tide was at its highest. In this analysis, the results reflected two types of waves: local wind-generated waves in the bay and open ocean waves originating from outside the bay. As the water depth in the innermost part of the bay is shallow (Fig. 1), high waves are attenuated by wave breaking. In addition, the width of the bay in the north-south direction is narrow and the fetch length is short, suggesting that large waves do not develop in the bay even when a typhoon approaches. As mentioned in Section 2.3, a breakwater was considered in the computation, resulting in short-wave periods behind this structure. Relatively long-period open ocean waves were blocked by the breakwater, and waves at the mangrove site were mainly accounted for by locally generated short waves.

Table 1 shows the predicted numerical values of each meteorological and hydrological parameter: tide, atmospheric pressure drop, storm surge, wind speed, current speed, wave height, and period for each two-hour period between 12:00 on September 5 and 6:00 on September 6. During this period, which was strongly affected by the typhoon (from 14:00 to 22:00 on September 5), the tide level was low. Even when considering storm surges caused by the pressure drop, the mangrove site was unlikely to be inundated. At 2:00 on September 5, the tide level rose to 83 cm at the site where planting took place, indicating that the water level was higher than the height of the young mangroves. However, the wave height at this time was as low as 5 cm; therefore, it is likely that the

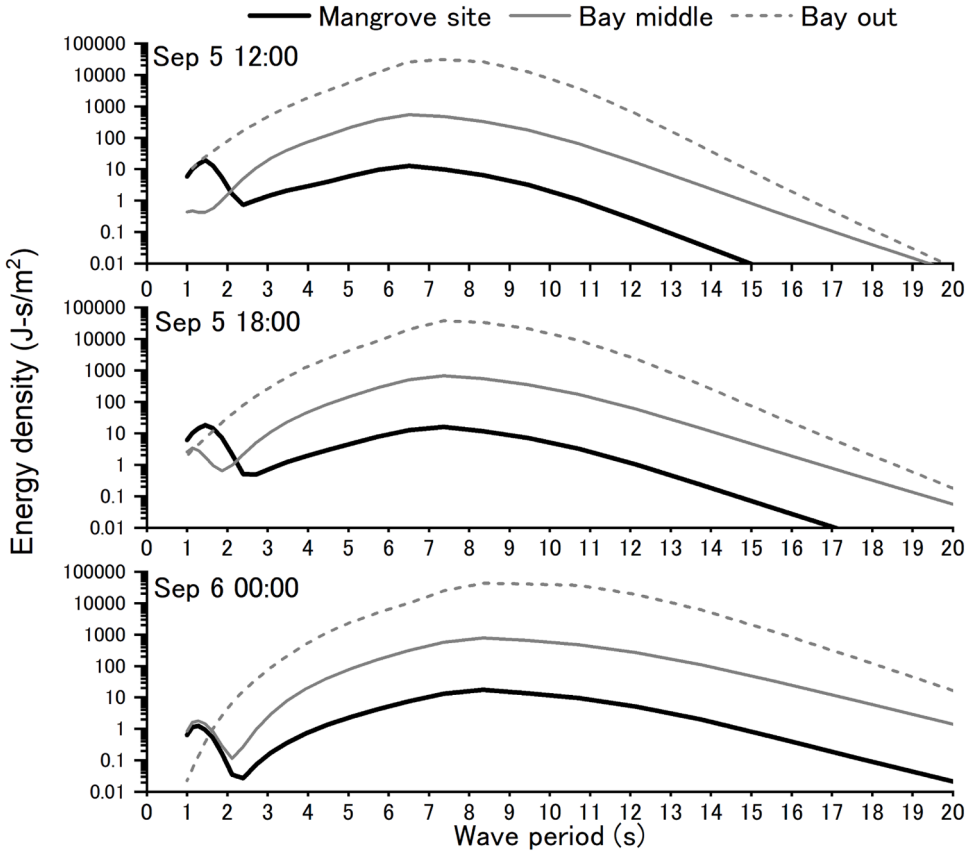

Fig. 11. Wave energy density at 12:00 and 18:00 on Sep 5 and 0:00 on Sep 6. At the mangrove forest in the far end of bay, there are two peaks of wave energy at two different periods. At 12:00 on Sep 5, the short-period peak is dominant, but at 00:00 on Sep 6, it shifts to the long-period side.

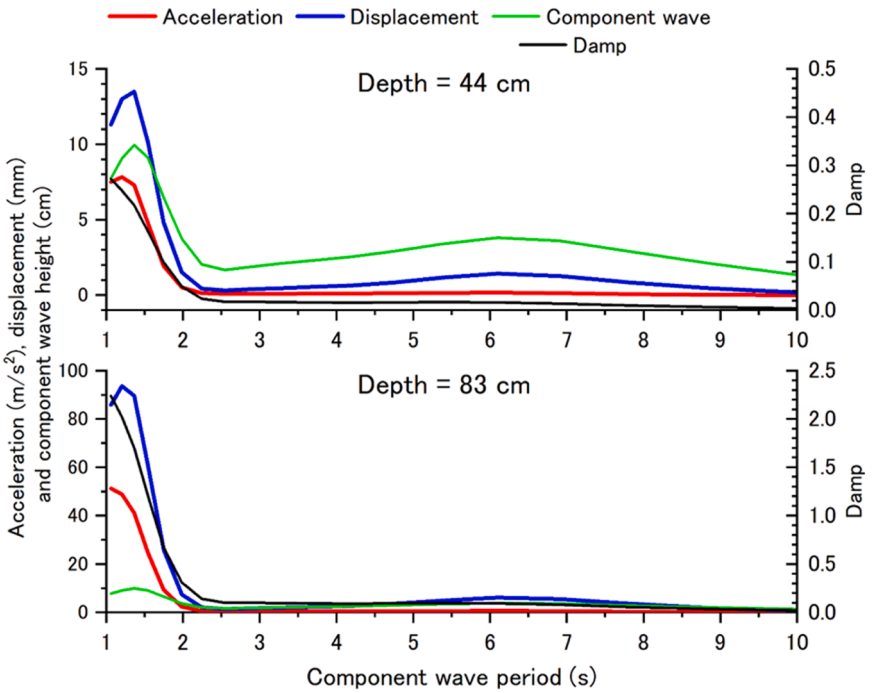

Fig. 12. Variation of oscillatory acceleration, horizontal displacement, the D_{amp} value of young mangrove, and wave height at different wave periods. Top: water depth = 44 cm (Sep 5, 12:00; Bottom: 83 cm (Sep 6, 2:00). The upper figure reproduces the condition during the approach of Typhoon Haishen, while the lower figure predicts the conditions with more adverse tidal level.

mangroves were not severely damaged.

3.4. Forces acting on young mangroves

During typhoons, three main forces act on mangroves: waves, currents, and wind. Table 2 lists the maximum horizontal forces and bending moments for 18 h during the passage of the typhoon'. The total of the three forces, calculated by a simple linear superposition, is also shown. In reality, wave, wind, and current forces act in different directions, but they may act in the same direction at any given moment. Therefore, the maximum combined force is considered in this study.

Among the three forces, the current-induced force was very small and unlikely to affect mangroves. Comparing waves and wind, the wind force was larger overall because the projected area of the leaves was much larger than that of the stems. In particular, the bending moments due to wind tend to be larger than those due to waves because of the longer arm length from the ground. In addition, when the ground level was higher than the water level, waves did not reach the mangroves. For this reason, the wave force was calculated to be zero owing to low tide during the particularly high wave period from 16:00 to 20:00 on September 5. Thus, recognizing that the wave force is significantly affected by the tide level is necessary. In contrast, the wind force acting on mangroves mainly depends on the strength, size, path, and direction of typhoons, which are independent of sea conditions. However, the time period from 0:00 to 4:00 on September 6 was at high tide, when the young mangroves were completely submerged in seawater, and in such a situation, wind had no effect.

4. Discussion

Table 2 demonstrates that the total force on young mangroves was mainly determined by the wind force during the typhoon, whereas the effect of the wave force was relatively small and the current-induced force was negligible. When the waves were high between 16:00 and 20:00 on September 5, the ground was exposed to low tide; thus, wave forces did not act. This may explain why young mangroves were not damaged. To determine the stability limits of young mangroves (*K. obovata*), Sreeranga et al. [46] conducted manual wave generation tests in the field and found that waves as high as 10 cm did not topple 6-month-old mangroves. Unlike mature mangroves, young mangroves are more flexible; hence, it is considered that waves up to 14 cm high during Typhoon Haishen were not large enough to damage young mangroves. However, even if the wave force is small, strong oscillations due to waves can cause damage to the leaves [56].

During the passage of Typhoon Haishen, the maximum wave force (0.54N, occurred at 12:00 on September 5, which was much smaller than the maximum wind force (1.47N at 20:00 on September 5. However, wind acts in one direction and, thus, does not work as a dynamic load, whereas waves act in a reciprocating motion; thus, dynamic motion must be considered. Fig. 11 shows the wave energy density (wave energy per unit sea surface area) at three points in the bay (Fig. 10) during typhoon passage. As shown in Table 1, the wave at the mangrove site was particularly short (1.44 s) at 12:00 on September 5. At this time, the spectrum at the mangrove site had a peak on the low-period side, while there was also a peak of energy at a relatively long period of 6–7 s, which appears to be propagated from the open ocean. Interestingly, which of the two peaks dominated depends on the time; for example, at 0:00 on September 6, the peak energy with a longer period was larger than that with a shorter period. Overall, short-period waves tended to occur in the innermost part of the bay, whereas long-period waves tended to occur in the center and outer parts of the bay.

In the design of coastal structures such as breakwaters and sea dikes, longer waves generally cause larger wave forces and are more critical to structural design than shorter waves. In contrast, the acceleration of the oscillations of the mangrove stems was greater for waves with shorter periods. Hence, the small and short waves in the innermost part of the bay may act better or worse in terms of the stability of young mangroves. Fig. 12 shows the numerical results of the mangrove oscillatory acceleration, horizontal displacement, and the D_{amp} values (oscillatory amplification ratio) calculated for each component wave deduced from the energy density at the mangrove site at 12:00 on September 5. The upper figure shows the result based on the tide level at this particular

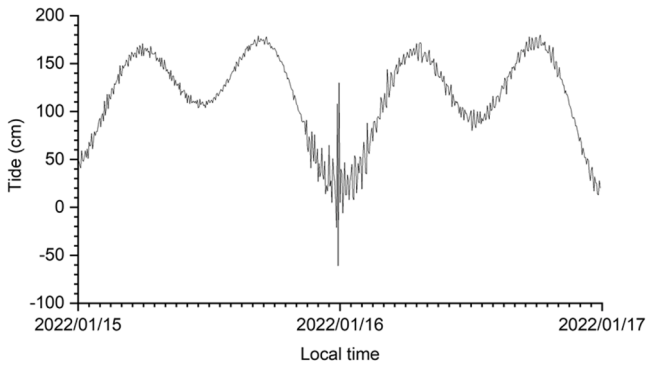

Fig. 13. Observed tidal level at the JMA Amami tide station (28°19′N and 129°32′E) when the 2022 Tonga tsunami arrived. Since the tsunami reached the site at low tide, the planted mangroves were probably unaffected.

time, whereas the lower figure shows a hypothetical result, which assumes that the values used for the wave height and period were the same as those of September 5 at 12:00, but the tide level was the same as that at 2:00 on September 6, when the tide was at its highest.

Both acceleration and displacement were found to have maximum values around the peak wave period (1.44 s). Mangrove oscillations respond to wave periods, making them more prone to shaking. Since the natural period of the young mangrove is assumed to be 0.36 s in this study, it is estimated that the mangrove strongly resonates with a wave energy component four times the natural period. The degree of resonance can also be confirmed from the D_{amp} values, which is 0.2 to 0.3 at a depth of 44 cm and around 2 at a depth of 83 cm, indicating that the degree of resonance is nearly 10 times different for a twofold difference in water depth. The maximum accelerations were approximately 8 m/s^2 at a depth of 44 cm and approximately 50 m/s^2 at a depth of 83 cm, which were 0.9 times and 5.1 times the gravitational acceleration, respectively.

Thus, young mangroves are more likely to resonate in deeper waters than in shallower waters, even at the same wave height and period. The stems of young mangroves are very flexible and are not likely to rupture; however, there is a possibility of damage to immature leaf parts if they are shaken strongly. Although relatively long waves with a period of 6–7 s also acted on the mangroves, the acceleration and displacement of the oscillations were small, and it is unlikely that they had a strong negative impact on young mangroves.

During the three-year period from May 2019 to May 2022, a small tsunami arrived on the island in January 2022 (Fig. 4). This tsunami was caused by atmospheric shock waves from the eruption of the volcanic island Hunga Tonga–Hunga Ha'apai, in the South Pacific, which triggered tsunami waves over a wide area of the world. A review of this event would be valuable for discussing the survival of mangroves in the event of a tsunami. The Tonga tsunami was widely monitored by a global network of coastal tide gauges, with notable tsunamis detected not only in the Pacific but also in the Atlantic and Indian oceans and the Caribbean and the Mediterranean seas [5]. This tsunami reached Japan much faster than typical tsunamis because it was caused by air pressure-forcing waves traveling at the speed of Lamb waves [19]. On Amami Island, short-period water-level fluctuations of approximately 1 m occurred 11 h after the eruption (Fig. 13). Although the impact of a 1-meter tsunami was not considered small, the survey conducted after the tsunami did not show any washaway of planted mangroves (Figs. 7 and 8). As shown in Fig. 13, the tsunami occurred at the lowest tide level, suggesting that its impact on mangroves may have been limited. In addition to typhoon events, the low tide level at the time of the tsunami may have positively contributed to the survival of the six young mangrove forests.

5. Broader implications of the results

Although this study only presents examples of one specific mangrove species (*K. obovata*) in a particular location (Amami Island, Japan), broader implications that may be useful for mangrove afforestation efforts could be derived from the present results, as follows:

- Mangrove propagules were planted directly at the seaward edge of the existing mangrove forest, and six of the seven plants grew well without loss. The main reasons for this success compared to the low success rate of mangrove planting shown in previous reports are considered to be the calm wave environment at the far end of the bay and the extensive deposition of fine sediments suitable for mangrove growth. In large-scale mangrove plantations, seedlings are usually grown in pods for several months and then transplanted to the planting site. The present results indicate that even direct planting, which seems disadvantageous to root development in the initial growth stage, may bring about a high success ratio if the environment is favorable. Given the growing concerns that plastic bags for mangrove saplings become marine wastes [20,60], it would be more environmentally friendly to plant mangroves directly where possible.
- In the present study, a strong typhoon approached 16 months after planting, but the young mangroves were able to survive. This result suggests that afforestation could be successful even in an environment subjected to tropical cyclones. However, if a typhoon were to approach two or three months after planting, it is questionable whether the planted mangroves would survive. Tidal conditions during storms are unpredictable but may strongly affect the success rate of mangrove planting. Wave heights tend to be large when the tide is high, while wave periods tend to be shortened in the inner part of the bay. Under such conditions, highly flexible young mangroves could be shaken strongly due to short-period choppy waves.
- As mentioned above, young mangroves may have difficulty adapting to the effects of short-period high waves under high tide conditions. This implies that if the sea level continues to rise, the conditions will become unfavorable for mangroves. However, the young mangroves in the present study were able to survive even under the conditions of being completely submerged by the daily tide. Therefore, sea-level rise will not immediately make mangrove planting impossible. Nevertheless, further research is needed on how to expand mangrove forests in response to long-term sea-level rise.
- The planting test conducted in this study was attempted in the natural environment. However, it was not completely natural, with a coastal road running behind the mangrove forest and a long breakwater at the mouth of the bay. These gray infrastructures may promote the deposition of fine sediment and contribute to increasing wave calmness, which is not necessarily negative for the growth of mangroves. Therefore, it is important to consider the synergistic, rather than just the conflicting, effects of green and gray infrastructures. This kind of constructive thinking will lead to appropriate usages of gray infrastructures such as a small breakwater to assist the growth of young mangroves.

6. Conclusion

The concepts of nature-based solutions, Eco-DRRs, and green infrastructure have attracted much attention in recent years as means of disaster mitigation; however, how to design such solutions against local external forces is not necessarily clear. In this study, a growth test of planted mangroves was conducted on Amami Island for three years. During this period, a strong typhoon approached the island 16 months after planting but six out of the seven planted mangroves survived. The external forces acting on young mangroves, such as waves, currents, and wind forces, caused by the typhoon were estimated to reveal why the young planted mangroves survived without being washed away. Wave

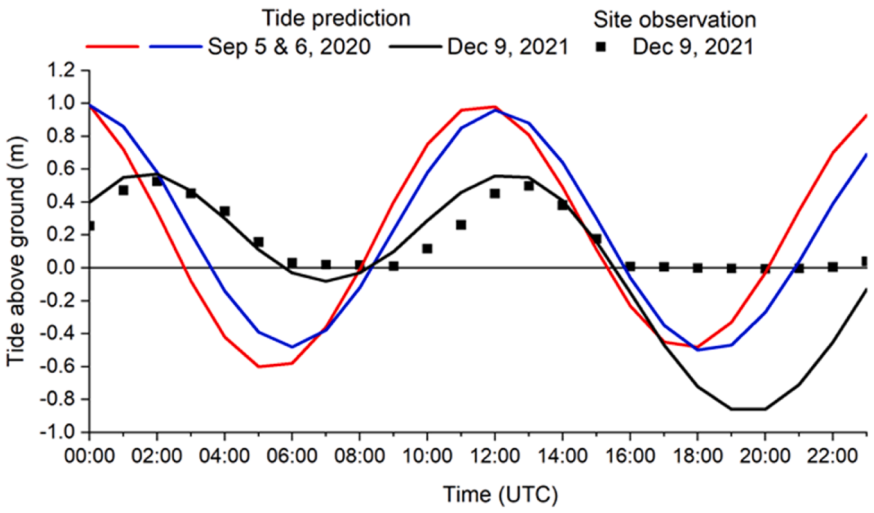

Fig. A1. Predicted tides when Typhoon Haishen approached the island in 2020.

height, flow velocity, and tidal level were not very high, and this may have allowed the survival of those young mangroves not yet strong. This study demonstrates that young mangroves can grow undamaged, despite the direct action of waves, currents, and winds, if the external forces acting on them are not too strong. This observation is encouraging for mangrove plantation activities in areas exposed to tropical cyclones. However, it was also found that the survival of mangroves was greatly affected by uncertainties, such as tide level, wave height and period, and wind direction at the time of the event. The predominance of short-period waves amplified the oscillations of young mangroves, and the horizontal acceleration during the typhoon was estimated to be almost equal to the gravitational acceleration. If the tidal level is slightly higher, much stronger oscillations, which can reach five times the gravitational acceleration, could damage mangrove leaves, even though the stems could respond flexibly. During the three-year period of the mangrove growth test, a one-meter tsunami generated by the volcanic eruption in Tonga also reached the island. However, there was no visible damage to the planted mangroves because the tide level was low enough at the time of tsunami arrival that it did not substantially affect the young mangroves. In this way, the young mangroves survived with a high success ratio thanks to various favorable conditions. It is expected that many more onsite observations will be collected in the future and used as a reference, leading to improved mangrove plantations or reliable mangrove protections in an engineered manner.

NBS impacts and implications

Young mangrove growth tests were conducted in a forest on Amami Island, Japan. Although affected by a strong typhoon, they survived for 36 months without damage. The offshore waves were over 10 m, but near the forest they were greatly attenuated. The low tide during high waves also contributed to survival of young mangroves. Short-period waves may have caused negative strong oscillations of young mangroves. Although this study only presents examples of specific mangrove species in a particular location, the findings are expected to provide a clue of how long young mangroves need to be protected in an engineered manner.

Declaration of Competing Interest

The authors declare that they have no known competing financial interests or personal relationships that could have appeared to influence the work reported in this paper.

Data availability

Data will be made available on request.

Acknowledgments

This research was funded by grants awarded to the Tokyo Institute of Technology (Japan Society for the Promotion of Science, 19K04964 and 23K04343). Field surveys on Amami Island were conducted with the help of former students of the corresponding author. The author would like to thank these former students, particularly Sindhu Sreeranga and Rikuo Shirai, for their cooperation.

Appendix A1. Tides in the forest of Amami Island

Although astronomical tides can be used to calculate the tide level in Sumiyo Bay during an approaching typhoon, the tidal data do not necessarily coincide with the land height. To match the elevation data, a pressure sensor (HOBO Water Level, Onset) was installed during the December 2021 field survey of the mangrove forest. Fig. A1 shows the calibrated tidal data with respect to the ground surface at the mangrove planting site. The tidal graphs for September 5 and 6, 2020, when Typhoon Haishen approached, indicate that the area was inundated by 1 m during high tide. Because the tidal level during this period was almost the highest in 2020, this location was potentially inundated by up to 1 m.

References

[1] D.M. Alongi, Mangrove forests: resilience, protection from tsunamis, and responses to global climate change, Estuarine, Coastal and Shelf Science, 76 (2008) 1–13.
[2] E.B. Barbier, Natural barriers to natural disasters: replanting mangroves after the tsunami, Frontiers in Ecology and the Environment 4 (3) (2006) 124–131.
[3] E.B. Barbier, S.D. Hacker, C. Kennedy, E.W. Koch, A.C. Stier, B.R. Silliman, The value of estuarine and coastal ecosystem services, Ecological Monographs 81 (2011) 139–193.
[4] M.A. Benedict, E. McMahon, Green Infrastructure: Smart Conservation for the 21st Century, Renewable Resources Journal (2002) 12–17.
[5] M. Carvajal, I. Sepúlveda, A. Gubler, R. Garreaud, Worldwide Signature of the 2022 Tonga Volcanic Tsunami, Geophysical Research Letters 49 (2022) e2022GL098153.
[6] A. Chausson, B. Turner, D. Seddon, N. Chabaneix, C.A.J. Girardin, V. Kapos, I. Key, D. Roe, A. Smith, S. Woroniecki, N. Seddon, Mapping the effectiveness of nature-based solutions for climate change adaptation, Global Change Biology 26 (2020) 6134–6155.
[7] J. Chow, Mangrove Management for Climate Change Adaptation and Sustainable Development in Coastal Zones, Journal of Sustainable Forestry 37 (2017) 139–156.

[8] N.T.K. Cuc, H.T. Hien, Stand structure and above ground biomass of Kandelia obovata Sheue, H.Y. Liu & J. Yong mangrove plantations in Northern, Viet Nam, Forest Ecology and Management 483 (2021), 118720.
[9] S. Das, Does mangrove plantation reduce coastal erosion? Assessment from the west coast of India, Regional Environmental Change 20 (2020) 58.
[10] A.O. Debrot, A. Plas, H. Boesono, K. Prihantoko, M.J. Baptist, A.J. Murk, F. H. Tonneijck, Early increases in artisanal shore-based fisheries in a Nature-based Solutions mangrove rehabilitation project on the north coast of Java, Estuarine, Coastal and Shelf Science 267 (2022), 107761.
[11] A. Dey, J.R.B. Alfred, B.R. Chowdhury, U. Censkowsky, Mangroves, as Shore Engineers, Are Nature-Based Solutions for Ensuring Coastal Protection, IN:. Handbook of Ecological and Ecosystem Engineering, Wiley, 2021, pp. 317–331.
[12] M. Doelle, T.G. Puthucherril, Nature-based solutions to sea level rise and other climate change impacts on oceanic and coastal environments: a law and policy perspective, Nordic Journal of Botany 2021 (2021) e03051.
[13] T. Dunlop, W Glamore, S. Felder, Restoring estuarine ecosystems using nature-based solutions: Towards an integrated eco-engineering design guideline, Science of The Total Environment 873 (2023), 162362.
[14] Environmental Justice Foundation, Mangroves: Nature's defence against Tsunamis—A report on the impact of mangrove loss and shrimp farm development on coastal defences, Environmental Justice Foundation, London, UK, 2006.
[15] C. Eckart, Surface waves on water of variable depth, Lecture Notes, Scripps Institution of Oceanography, University of California, 1951.
[16] C. Elster, Reasons for reforestation success and failure with three mangrove species in Colombia, Forest Ecology and Management 131 (2000) 201–214.
[17] S.E. Hamilton, D. Casey, Creation of a high spatio-temporal resolution global database of continuous mangrove forest cover for the 21st century (CGMFC-21), Global Ecology and Biogeography 25 (2016) 729–738.
[18] K. Hasselmann, T.P. Barnett, E. Bouws, H. Carlson, D.E. Cartwright, K. Enke, J. Ewing, H. Gienapp, D.E. Hasselmann, P. Kruseman, A. Meerburg, P. Müller, D. J. Olbers, K. Richter, W. Sell, H. Walden, Measurements of wind-wave growth and swell decay during the Joint North Sea Wave Project (JONSWAP), Deutsche Hydrographische Zeitschrift 8 (12) (1973).
[19] T-C. Ho, N. Mori, Ocean gravity waves generated by the meteotsunami at the Japan Trench following the 2022 Tonga volcanic eruption, Eatyh, Plantets and Space 75 (1) (2023) 1–10.
[20] J. Holbert, D.J. Sudrajat, Yulianti Nurhasybi, Alternative methods for reforestation and land rehabilitation to reduce the plastics waste in forest areas, IOP Conference Series: Earth and Environmental Science 407 (2019), 012007.
[21] IFRC, Breaking the waves: Impact analysis of coastal afforestation for disaster risk reduction in Viet Nam, International Federation of Red Cross and Red Crescent Societies, Geneva, 2011.
[22] IUCN, in: E.G. Cohen-Shacham, C.J. Walters, S. Maginnis (Eds.), Nature-based Solutions to address global societal challenges, IUCN, Gland, Switzerland, 2016, p. 97. Switzerland.
[23] JICA, Technical Document 3 Mangrove Plantation Guideline, The Qurm Environmental Information Center Project, 2014.
[24] Japan Meteorological Agency, Outline of the operational numerical weather prediction, 2019. https://www.jma.go.jp/jma/jma-eng/jma-center/nwp/outline2019-nwp/index.htm. accessed on March 20, 2023.
[25] Japan Meteorological Agency, Climate change monitoring report 2021, 2022, p. 89.
[26] B. Kamali, R. Hashim, Mangrove restoration without planting, Ecological Engineering 37 (2011) 387–391.
[27] K. Kathiresan, N. Rajendran, Coastal mangrove forests mitigated tsunami, Estuarine, Coastal and Shelf Science 65 (2005) 601–606.
[28] K.A.S. Kodikara, N. Mukherjee, L.P. Jayatissa, F. Dahdouh-Guebas, N. Koedam, Have mangrove restoration projects worked? An in-depth study in Sri Lanka, Restoration Ecology 25 (2017) 705–716.
[29] N. Kumano, M. Tamura, T. Inoue, H. Yokoki, Estimating the cost of coastal adaptation using mangrove forests against sea level rise, Coastal Engineering Journal 63 (2021) 263–274.
[30] W.K. Lee, S.H.X. Tay, S.K. Ooi, D.A. Friess, Potential short wave attenuation function of disturbed mangroves, Estuarine, Coastal and Shelf Science 248 (2020), 106747.
[31] R.R. Lewis, Ecological engineering for successful management and restoration of mangrove forests, Ecological Engineering 24 (4) (2005) 403–418.
[32] W. Ma, W. Wang, C. Tang, G. Chen, M. Wang, Zonation of mangrove flora and fauna in a subtropical estuarine wetland based on surface elevation, Ecology and Evolution 10 (14) (2020) 7404–7418.
[33] F. Meulen, S. Ijff, R. Zetten, Nature-based solutions for coastal adaptation management, concepts and scope, an overview, Nordic Journal of Botany 2023 (1) (2022) e03290.
[34] T. Mikami, T. Shibayama, H. Takagi, R. Matsumaru, M. Esteban, N.D. Thao, M. de Leon, V.P. Valenzuela, T. Oyama, R. Nakamura, K. Kumagai, S. Li, Storm Surge Heights and Damage Caused by the 2013 Typhoon Haiyan Along the Leyte Gulf Coast, Coastal Engineering Journal 58 (1) (2016) 27, 1640005.
[35] Ministry of the Environment, Ecosystem-based Disaster Risk Reduction in Japan: A handbook for practitioners, 2016, p. 18.
[36] J.M. Montgomery, K.R. Bryan, J.C. Mullarney, E.M. Horstman, Attenuation of Storm Surges by Coastal Mangroves, Geophysical Research Letters 46 (5) (2019) 2680–2689.
[37] Y. Moriizumi, N. Matsui, H. Hondo, Simplified life cycle sustainability assessment of mangrove management: a case of plantation on wastelands in Thailand, Journal of Cleaner Production 18 (2010) 1629–1638.
[38] V.A. Myers, Characteristics of United States hurricanes pertinent to levee design for lake Okeechobee, Florida, Hydrometeorological Report, US Weather Bureau, 1954, p. 106. No. 32.
[39] D.T. Nguyen, H. Takagi, M. Esteban (Eds.), Coastal Disasters and Climate Change in Vietnam: Engineering and Planning Perspectives, Elsevier, 2014, p. 424.
[40] T.P. Nguyen, N.V. Tam, L.P. Quoi, K.E. Parnell, Community perspectives on an internationally funded mangrove restoration project: Kien Giang province, Vietnam, Ocean & Coastal Management 119 (2016) 146–154.
[41] C.T. Perry, A. Berkeley, Intertidal substrate modification as a result of mangrove planting: Impacts of introduced mangrove species on sediment microfacies characteristics, Estuarine, Coastal and Shelf Science 81 (2008) 225–237.
[42] J.H. Primavera, J.M.A. Esteban, A review of mangrove rehabilitation in the Philippines: Successes, failures and future prospects, Wetlands Ecology and Management 16 (2008) 345–358.
[43] T. Rasmeemasmuang, J. Sasaki, Wave Reduction in Mangrove Forests: General Information and Case Study in Thailand, IN: Handbook of Coastal Disaster Mitigation for Engineers and Planners, Elsevier, 2015, pp. 511–535.
[44] D.R. Richards, D.A. Friess, Rates and drivers of mangrove deforestation in Southeast Asia, 2000–2012, Proceedings of the National Academy of Sciences 113 (2) (2015) 344–349.
[45] R.W. Schloemer, Analysis and synthesis of hurricane wind patterns over Lake Okeechobee, Florida, 1954. Hydrometerorological Report No. 31.
[46] S. Sreeranga, H. Takagi, R. Shirai, Community-Based Portable Reefs to Promote Mangrove Vegetation Growth: Bridging between Ecological and Engineering Principles, International Journal of Environmental Research and Public Health, MDPI, 18 (2021) 590.
[47] S. Sreeranga, H. Takagi, S. Kubota, J. Mitsui, An experimental study on oscillatory characteristics of young mangroves behind a portable reef, Coastal Engineering Journal 65 (1) (2022) 110–125.
[48] H. Takagi, S. Li, M. de Leon, M. Esteban, T. Mikami, R. Matsumaru, T. Shibayama, R. Nakamura, Storm surge and evacuation in urban areas during the peak of a storm, Coastal Engineering 108 (2016) 1–9.
[49] H. Takagi, W. Wu, Maximum wind radius estimated by the 50 kt radius: improvement of storm surge forecasting over the western North Pacific, Natural Hazards and Earth System Sciences, European Geosciences Union 16 (2016) 705–717.
[50] H. Takagi, M. Esteban, T. Shibayama, T. Mikami, R. Matsumaru, M.D. Leon, N. D. Thao, T. Oyama, R. Nakamura, Track analysis, simulation, and field survey of the 2013 Typhoon Haiyan storm surge, J. Flood Risk Management 10 (1) (2017) 42–52.
[51] H. Takagi, Long-Term Design of Mangrove Landfills as an Effective Tide Attenuator under Relative Sea-Level Rise, Sustainability 10 (2018) 1045.
[52] H. Takagi, Y. Xiong, F. Furukawa, Track analysis and storm surge investigation of 2017 Typhoon Hato: were the warning signals issued in Macau and Hong Kong timed appropriately? Georisk 12 (2018) 297–307.
[53] H. Takagi, Adapted mangrove on hybrid platform" – Coupling of ecological and engineering principles against coastal hazards, Results in Engineering 4 (2019) 6.
[54] H. Takagi, N.H. Quan, L.T. Anh, N.D. Thao, V.P.D. Tri, T.T. Anh, Practical Modelling of Tidal Propagation under Fluvial Interaction in the Mekong Delta, International Journal of River Basin Management 17 (3) (2019) 377–387.
[55] H. Takagi, S. Sekiguchi, N.D. Thao, T. Rasmeemasmuang, Do wooden pile breakwaters work for community-based coastal protection? Journal of Coastal Conservation 24 (31) (2020) 11.
[56] H. Takagi, R. Shirai, S. Sreeranga, Oscillatory characteristics of young mangroves exposed to short-period waves, Science of The Total Environment 790 (2021), 148157.
[57] H. Takagi, A. Takahashi, Short-fetch high waves during the passage of 2019 Typhoon Faxai over Tokyo Bay, Frontiers of Earth Science 15 (2) (2022) 206–219.
[58] H. Takagi, L.T. Anh, M.R. Islam, T.T. Hossain, Progress of Disaster Mitigation Against Tropical Cyclones and Storm Surges: A Comparative Study of Bangladesh, Vietnam, and Japan, Coastal Engineering Journal 65 (1) (2023) 39–53.
[59] S. Temmerman, E.M. Horstman, K.W. Krauss, J.C. Mullarney, I. Pelckmans, K. Schoutens, Marshes and Mangroves as Nature-Based Coastal Storm Buffers, Annual Review of Marine Science (2023).
[60] A. Thampi, B. Vedharajan, S. Narayana, Govindarajan, R Magalingam, Experiment on use of eco-friendly Palmyra nursery bag for mangrove restoration in Palk Bay, India, Restoration Ecology 15 (2023) 95–118.
[61] N.D. Thao, H. Takagi, M. Esteban (Eds.), Coastal Disasters and Climate Change in Vietnam: Engineering and Planning Perspectives, Elsevier, 2014, p. 424.
[62] B.S. Thompson, The political ecology of mangrove forest restoration in Thailand: Institutional arrangements and power dynamics, Land Use Policy 78 (2018) 503–514.
[63] TU Delft SWAN Cycle III Version 40.11 User Manual., 2000.
[64] C.E.J. van Bijsterveldt, B.K. van Wesenbeeck, S. Ramadhani, Raven Ol.V . , F. E. van Gool, R. Pribadi, T.J Bouma, Does plastic waste kill mangroves? A field experiment to assess the impact of macro plastics on mangrove growth, stress response and survival, Science of The Total Environment 756 (2021), 143826.
[65] B.M.R. Villamayor, R.N. Rollon, M.S. Samson, G.M.G. Albano, J.H. Primavera, Impact of Haiyan on Philippine mangroves: Implications to the fate of the widespread monospecific Rhizophora plantations against strong typhoons, Ocean and Coastal Management 132 (2016) 1–14.
[66] J.C. Winterwerp, T. Albers, E.J. Anthony, D.A. Friess, A.G. Mancheño, K. Moseley, A. Muhari, S. Naipal, J. Noordermeer, A. Oost, C. Saengsupavanich, S.A.J. Tas, F. H. Tonneijck, T. Wilms, C. Van Bijsterveldt, P. Van Eijk, E. Van Lavieren, B.K. Van

Wesenbeeck, Managing erosion of mangrove-mud coasts with permeable dams – lessons learned, Ecological Engineering 158 (2020), 106078.
[67] J. Wilchcombe, R. Nishi, J. Simmons, M. Widlansky, Y. Tsurunari, Field survey on storm surge by catastrophic Hurricane Dorian in the Bahamas 2019, Journal of Japan Society of Civil Engineers, Ser. B3 (Ocean Engineering) 77 (2) (2021). I_289–I_294.
[68] Z. Zhang, V.P. Chua, H.F. Cheong, Hydrodynamics in mangrove prop roots and their physical properties, Journal of Hydro-environment Research 9 (2) (2015) 281–294.